INFLUENCE OF IONOSPHERE PERTURBATIONS IN GPS TIME AND FREQUENCY TRANSFER

Sophie Pireaux, Pascale Defraigne, Nicolas Bergeot,
Quentin Baire, and Carine Bruyninx
Royal Observatory of Belgium
Avenue Circulaire, 3, B-1180 Brussels, Belgium
E-mail: *sophie.pireaux@oma.be*

Abstract

The stability of GPS time and frequency transfer is limited by the fact that GPS signals travel through the ionosphere. In high-precision geodetic time transfer (i.e. based on precise modelling of code and carrier-phase GPS data), the so-called ionosphere-free combination of the code and carrier-phase measurements made on the two frequencies is used to remove the first-order ionosphere effect. In this paper, we investigate the impact of residual second- and third-order ionosphere perturbations on geodetic time transfer solutions, using the ATOMIUM software developed at the Royal Observatory of Belgium (ROB). The impact of third-order ionosphere effects was shown to be negligible, while for second-order effects, the tests performed on different time links and at different epochs show a small effect of the order of some picoseconds, on a quiet day, and up to more than 10 picoseconds in case of high ionosphere activity.

INTRODUCTION

Time and frequency transfer (TFT) using GNSS satellites is widely used within the time community, for example for the realization of TAI (Temps Atomique International), the basis of the legal time UTC (Universal Time Coordinated), computed by the Bureau International des Poids et Mesures (BIPM). TFT is characterized by its very good resolution (1 observation point/30s or possibly 1 point per second) and a high precision and frequency stability thanks to the carrier phases (uncertainty uA of about 0.1 ns). The present uncertainty in GPS equipment calibration is 5 ns (uncertainty uB – systematics, hence calibration errors – in the BIPM Circular T). Since ionosphere perturbations on electromagnetic waves are frequency dependent and since GPS signals are broadcast in two different frequencies, ionosphere effects are commonly removed through a given combination (named ionosphere-free) of the signals in the two frequencies f_1 and f_2. However, it is well known that this combination removes only first-order perturbations, which correspond to about 99.9% of the total perturbation. The present study aims at evaluating the impact of the remaining part, concentrating on second- and third-order effects. These higher-order terms are, therefore, implemented in the software ATOMIUM **[1]**, developed at the Royal Observatory of Belgium. ATOMIUM is based on a least-squares analysis of dual-frequency carrier-phase and code measurements and is able to provide clock solutions in Precise Point Positioning (PPP), as well as in single difference (also called Common View, CV) mode.

The present paper is organized as follows. The first section recalls the principles of GPS TFT and the ionosphere-free analysis in Precise Point Positioning or Common View mode. In Section 2, the ionosphere-free analysis, as implemented in the ATOMIUM software, is reviewed. Then, the Slant Total Electron Content (TEC) is defined in Section 3, which also summarizes TEC relevance to ionosphere perturbations. In Section 4, the selected method used to implement higher-order ionosphere corrections in ATOMIUM ionosphere-free analysis is described. Our corresponding results are presented in Section 5, in terms of ionosphere delays of second and third orders compared to first-order ionosphere effect, and then in terms of the impact of higher-order ionosphere delays in the receiver clock solution computed with ATOMIUM. This section also provides a discussion about the use of reprocessed satellite orbits, accounting for high-order ionosphere corrections. Some conclusions are finally presented in Section 6.

1. GEODETIC TFT AND IONOSPHERE IN GPS SIGNALS

For a station p or similarly q, the GPS measurements, relative to observed satellite i, on the signal code P_k and phase L_k , at frequency k (1 for f_1=1575.42 MHz or 2 for f_2=1227.6 MHz) with corresponding wavelength λ_k , can be written in length units as

$$(\boldsymbol{P_k})^{\boldsymbol{i}}_{\boldsymbol{p}} = \boldsymbol{\rho}^{\boldsymbol{i}}_{\boldsymbol{p}} + \boldsymbol{c}\Delta\boldsymbol{t}_{\boldsymbol{p}} + \boldsymbol{c}\Delta\boldsymbol{\tau}^{\boldsymbol{i}} + \boldsymbol{zpd}_{\boldsymbol{p}} + \boldsymbol{\varepsilon}_{\boldsymbol{P}} + \left(+\boldsymbol{I1}_{\boldsymbol{k}} + 2\cdot\boldsymbol{I2}_{\boldsymbol{k}} + 3\cdot\boldsymbol{I3}_{\boldsymbol{k}}\right)^{\boldsymbol{i}}_{\boldsymbol{p}} \quad (1a)$$

$$(\boldsymbol{L_k})^{\boldsymbol{i}}_{\boldsymbol{p}} = \boldsymbol{\rho}^{\boldsymbol{i}}_{\boldsymbol{p}} + \boldsymbol{c}\Delta\boldsymbol{t}_{\boldsymbol{p}} + \boldsymbol{c}\Delta\boldsymbol{\tau}^{\boldsymbol{i}} + \boldsymbol{zpd}_{\boldsymbol{p}} + \boldsymbol{N}^{\boldsymbol{i}}_{\boldsymbol{p}}\boldsymbol{\lambda}_{\boldsymbol{k}} + \boldsymbol{\varepsilon}_{\boldsymbol{L}} + \left(-\boldsymbol{I1}_{\boldsymbol{k}} - \boldsymbol{I2}_{\boldsymbol{k}} - \boldsymbol{I3}_{\boldsymbol{k}}\right)^{\boldsymbol{i}}_{\boldsymbol{p}} \quad (1b)$$

where ρ^i_p is the geometric distance i-p ; Δt_p is the station clock synchronization error; $\Delta\tau^i$ is the satellite clock synchronization error; zpd_p is the troposphere path delay for station p; $I1_k$, $I2_k$ and $I3_k$ are ionosphere first-, second-, and third-order delays on frequency k; N^i_p are phase ambiguities; ε_P and ε_L are the error terms in code and phase, containing noise and multipath.

When a dual-frequency GPS receiver is available at station p, the so-called ionosphere-free combination (k=3) is used:

$$\boldsymbol{P}_3 = \frac{\boldsymbol{f}_1^{\,2}}{(\boldsymbol{f}_1^{\,2} - \boldsymbol{f}_2^{\,2})}\boldsymbol{P}_1 - \frac{\boldsymbol{f}_2^{\,2}}{(\boldsymbol{f}_1^{\,2} - \boldsymbol{f}_2^{\,2})}\boldsymbol{P}_2 \quad (2a)$$

$$\boldsymbol{L}_3 = \frac{\boldsymbol{f}_1^{\,2}}{(\boldsymbol{f}_1^{\,2} - \boldsymbol{f}_2^{\,2})}\boldsymbol{L}_1 - \frac{\boldsymbol{f}_2^{\,2}}{(\boldsymbol{f}_1^{\,2} - \boldsymbol{f}_2^{\,2})}\boldsymbol{L}_2 \quad (2b)$$

with f_1 and f_2 the two GPS carrier frequencies. This combination removes, from the GPS signal, the first-order ionosphere effect, $I1$, since the latter is proportional to the inverse of the square frequency.

The corresponding ionosphere-free observation equations therefore do not contain any first-order ionosphere term, but new factors for second- and third-order ionosphere effects with respect to the previous Equation (1):

$$(\boldsymbol{P}_3)^{\boldsymbol{i}}_{\boldsymbol{p}} = \boldsymbol{\rho}^{\boldsymbol{i}}_{\boldsymbol{p}} + \boldsymbol{c}\Delta\boldsymbol{t}_{\boldsymbol{p}} + \boldsymbol{c}\Delta\boldsymbol{\tau}^{\,i} + \boldsymbol{zpd}_{\boldsymbol{p}} + \boldsymbol{\varepsilon}_{\boldsymbol{P}} + \left(+2\cdot\boldsymbol{I2}_3 - 3\cdot\boldsymbol{I3}_3\right)^{\boldsymbol{i}}_{\boldsymbol{p}} \quad (3a)$$

$$(\boldsymbol{L}_3)^{\boldsymbol{i}}_{\boldsymbol{p}} = \boldsymbol{\rho}^{\boldsymbol{i}}_{\boldsymbol{p}} + \boldsymbol{c}\Delta\boldsymbol{t}_{\boldsymbol{p}} + \boldsymbol{c}\Delta\boldsymbol{\tau}^{\,i} + \boldsymbol{zpd}_{\boldsymbol{p}} + \boldsymbol{N}^{\boldsymbol{i}}_{\boldsymbol{p}}\boldsymbol{\lambda}_3 + \boldsymbol{\varepsilon}_{\boldsymbol{L}} + \left(-\boldsymbol{I2}_3 + \boldsymbol{I3}_3\right)^{\boldsymbol{i}}_{\boldsymbol{p}} \quad (3b)$$

Note that about 99.9% **[9]** of ionosphere perturbations are removed with $I1$ in the so-called ionosphere-free combination. Note also that while the first order has the same magnitude on GPS phase and code measurements (but with opposite sign), the impact of second- and third-orders effects is larger on code than on phase observations (twice for $I2$, three times for $I3$).

GPS observations and their modeling given by Equations (3a) and (3b) are directly used in Precise Point Positioning. For Common-View analysis, i.e. using the single differences between simultaneous observations of a same satellite *i* in two remote stations *p* and *q* in order to determine directly the synchronization error between the two remote clocks, the observation equations for receivers *p* and *q* with satellite *i* are subtracted. This single difference cancels the satellite clock bias in the GPS signal, assuming that the nominal times of observation of the satellite by the two stations are the same.

When forming ionosphere-free combinations, the single-difference code and carrier-phase equations are:

$$(\boldsymbol{P}_3)^{i}_{pq} = \boldsymbol{\rho}^{i}_{pq} + \boldsymbol{c}\Delta\boldsymbol{t}_{pq} + \boldsymbol{zpd}_{pq} + \boldsymbol{\varepsilon}_{P} + \left(+2\cdot\boldsymbol{I}2_3 - 3\cdot\boldsymbol{I}3_3\right)^{i}_{pq} \tag{4a}$$

$$(\boldsymbol{L}_3)^{i}_{pq} = \boldsymbol{\rho}^{i}_{pq} + \boldsymbol{c}\Delta\boldsymbol{t}_{pq} + \boldsymbol{zpd}_{pq} + \boldsymbol{N}^{i}_{pq}\boldsymbol{\lambda}_3 + \boldsymbol{\varepsilon}_{L} + \left(-\boldsymbol{I}2_3 + \boldsymbol{I}3_3\right)^{i}_{pq} \tag{4b}$$

where, for any quantity *X*,

$$\boldsymbol{X}_{pq} \equiv \boldsymbol{X}_{p} - \boldsymbol{X}_{q} \tag{5}$$

Now, all the terms in above Equations (1), (3), or (4) can be estimated via an inversion procedure using some *a priori* precise satellite orbits and satellite clock products. This finally provides the solution for either Δt_p in PPP, i.e. the clock synchronization error between the atomic clock connected to the GPS receiver and the IGS Time scale at each epoch, or Δt_{pq} in common view, i.e. the synchronization error between the remote clocks connected to two GPS receivers. In parallel, the station position and troposphere zenith delays are estimated as a by-product.

2. THE ATOMIUM SOFTWARE

The present study on ionosphere higher-order perturbations in TFT is based on the ATOMIUM software **[1]**, developed at the Royal Observatory of Belgium. ATOMIUM uses a weighted least-squares approach with ionosphere-free combinations of dual-frequency GPS code (P_3) and carrier-phase (L_3) observations. ATOMIUM was initially developed to perform GPS *PPP* and later adapted to single differences, or Common View (CV), of GPS code and carrier-phase observations. In the paragraphs below, we describe ATOMIUM, following the diagram presented in Figure 1.

When running ATOMIUM, GPS ionosphere-free code and phase combinations are constructed according to Equations (2, 6) from L_1, P_1, L_2, P_2 observations read in RINEX files. By default, the ATOMIUM software uses as *a priori* the International GNSS Service (IGS) products **[2]**. IGS satellite clocks (tabulated with a 5-minute interval) are used to obtain $\Delta\tau^{i}$ at the same sampling rate as provided. IGS satellite orbits (tabulated with a 15-minute interval) are used to estimate $\rho_p{}^{i}$ (or $\rho_{pq}{}^{i}$) via a 12-point Neville interpolation of the satellite position every 5 minutes.

The station position is corrected for its time variations due to degree 2 and 3 solid Earth tides as recommended by the IERS conventions **[3]** and for ocean loading according to the FES2004 model **[4]**. The relative (if GPS observations were made before GPS week 1400) or absolute (if after) elevation- (no azimuth) and nadir-dependant corrections for receiver and satellite antenna phase center variations are read from IGS *atx* file available at **[5]**.

Prior to the least-squares inversion, the computed geometric distance is removed from both phase and code ionosphere-free combinations. Those are also corrected for a relativistic (periodic only) delay and a troposphere delay. Troposphere delays are modeled as the sum of a hydrostatic and a wet delay, resulting

from the product of a given mapping function and of the corresponding hydrostatic or wet zenith path delay (*zpd*). For the hydrostatic part, we use the Saastamoien a priori model **[6]** and the dry Niell mapping function **[7]**. For the wet part, we use the wet Niell mapping function **[7]**, while the wet *zpd* is estimated as one point every 2 hours, and modeled by linear interpolation between these points.

Carrier-phase measurements are further corrected for phase windup **[8]**, taking into account satellite altitude and eclipse events.

The implementation of additional higher-order ionosphere corrections on phase and code is done at this level, as corrections applied on the code and phase measurements.

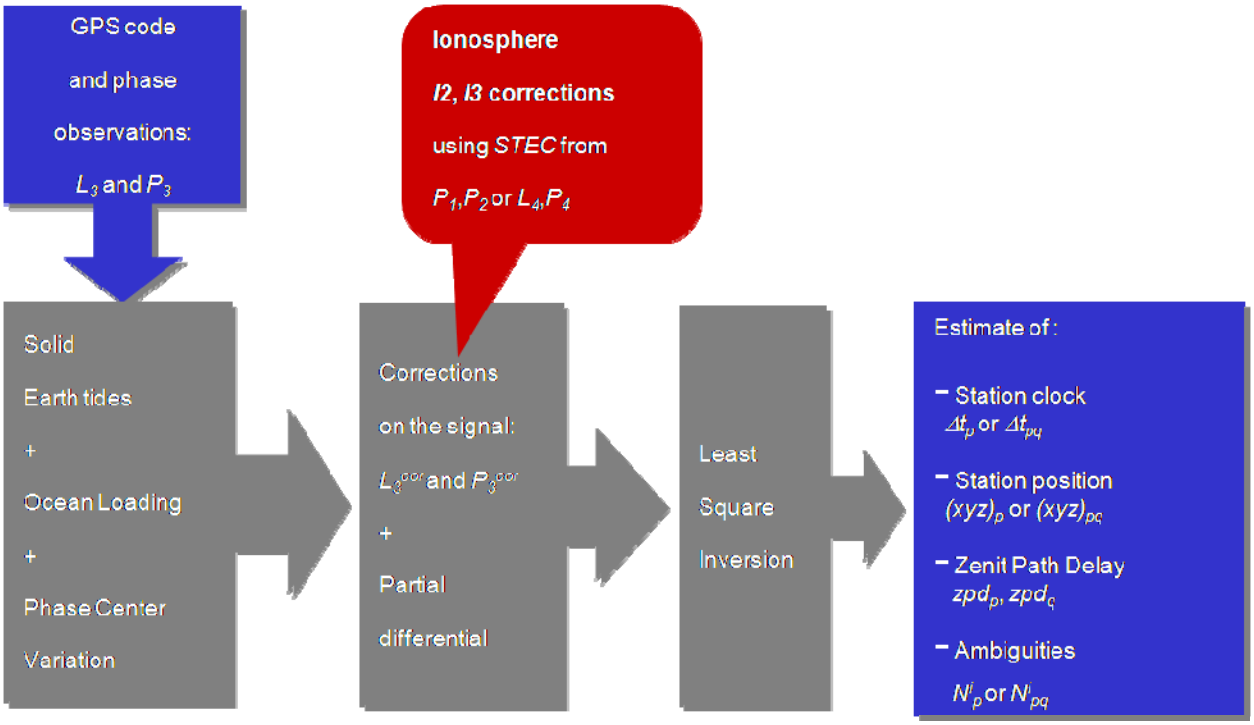

Figure 1. ATOMIUM software diagram.

The least-squares analysis used in ATOMIUM is detailed in Reference **[1]**.

As output, ATOMIUM provides the station *p* (or relative *p*-*q*) position for the whole day, the receiver clock *p* (or relative *p*-*q*) synchronization error every 5 minutes, and troposphere wet zenith path delays *p* (and *q*) at a given rate (2 hours in our case). Furthermore, the ionosphere Slant Electron Content (STEC) is computed from dual-frequency measurements (see Section 4) for each satellite-station pair with a sampling rate of 5 minutes.

3. RELEVANCE OF STEC FOR IONOSPHERE PERTURBATIONS

A good indicator of the state of the ionosphere is the Total Electron Content (TEC), which is the integrated electron density inside a cylinder column of unit base area along a certain direction between Earth ground and satellite altitude. Slant TEC (*STEC*) is taken along the satellite *i*- station *p* direction.

STEC is function not only of the satellite elevation or station position, but also of the time of the day, of the time of the year, of the solar cycle, and of the ionosphere particular conditions (as seen in Figure 2b during the ionosphere storm of November 30, 2003 for stations BRUS, i.e. Brussels, at latitude 50°28' and longitude 4°12', OPMT, i.e. Paris at latitude 48°30' and longitude 2°12', ONSA i.e. Onsala at latitude 57°14' and longitude 11°33'). Hence, GNSS ionosphere-induced errors will increase in the next few years due to the increasing solar activity associated with the ascending phase of the 24th sunspot cycle (maximum forecast around 2011-2012 depending on the model). Ionosphere effects in GPS (*I1, 12* and *I3*) are directly proportional to *STEC.*

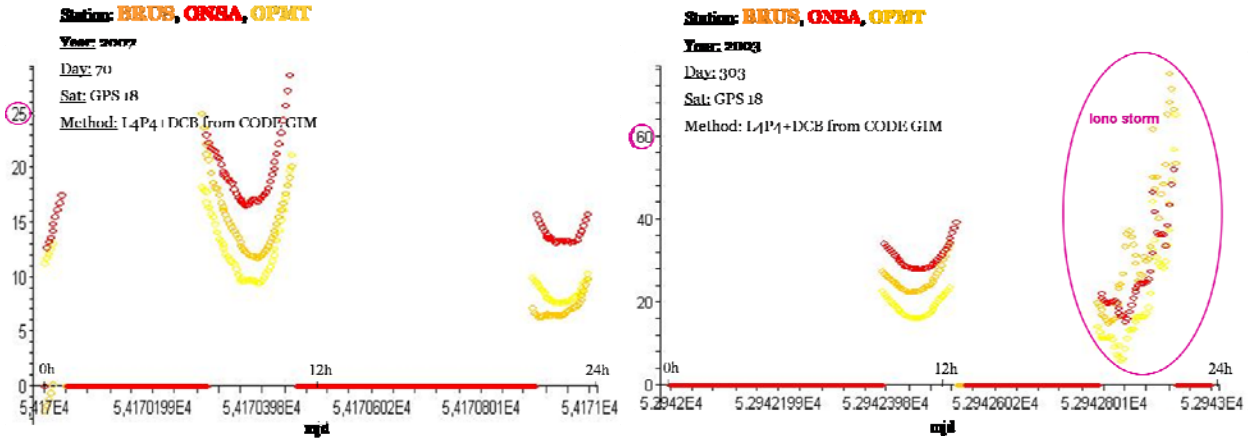

Figure 2. STEC above Brussels, Onsala and Paris stations a) on an ionosphere-quiet day (left) or b) on a stormy day (left). 1 TECU=10^{16} e^-/m^2.

4. METHOD TO CORRECT IONOSPHERE PERTURBATIONS FOR FREQUENCY *K*

As the *I1* term contains 99.9% of the ionosphere perturbations on GNSS signal, it can be used to estimate *STEC*. The second- and third-order terms, also directly proportional to *STEC*, are then computed using this estimated *STEC*.

The *STEC* in *I1* can be determined using the geometry-free combination (*noted as P_4 and L_4*). The latter only contains a given combination of ionosphere perturbations on f_1 and f_2 signals, some constant terms associated with the differential hardware delays in the satellite and in the receiver, plus the phase ambiguities:

$$P_4 = -P_1 + P_2 \tag{4a}$$

$$L_4 = L_1 - \frac{f_1}{f_2} L_2 \tag{4b}$$

Note that the bending effect is neglected in the present study, meaning that the trajectory considered to compute those ionosphere corrections on GPS observations is a straight line from satellite *i* to station *p* (and *q*).

FIRST-ORDER IONOSPHERE PERTURBATIONS

The first-order ionosphere effect, is given by **[10]**

$$\boldsymbol{I1_k = \alpha 1_k \cdot STEC} \tag{12a}$$

with the factor for GPS frequencies 1 and 2 being

$$\alpha 1_{1,2} = +\frac{40.3}{f_{1,2}^{\ 2}} \tag{12b}$$

This implies that the corresponding factors for the ionosphere-free (*k=3*) or geometry-free (*k=4*) combinations are

$$\alpha 1_3 = 0 \qquad\qquad \alpha 1_4 = -40.3 \cdot \left(\frac{1}{f_1^{\ 2}} - \frac{1}{f_2^{\ 2}} \right) \tag{12c}$$

As stated here above, for each pair of code or phase measurements (on f_1 and f_2), the geometry-free combination can be used to compute the *STEC* **[11]**, which is needed in higher-order ionosphere corrections. Neglecting the *I2* and *I3* contributions inducing errors in estimated *STEC* of the order of 0.1 TECU at the most, one gets:

$$\left(\boldsymbol{STEC}\right)^{\boldsymbol{i}}_{\boldsymbol{p}} = \frac{1}{\alpha 1_4} \left[\left(\boldsymbol{L}_4\right)^{\boldsymbol{i}}_{\boldsymbol{p}} - \left\langle \left(\boldsymbol{L}_4\right)^{\boldsymbol{i}}_{\boldsymbol{p}} - \left(\boldsymbol{P}_4\right)^{\boldsymbol{i}}_{\boldsymbol{p}} \right\rangle_{\substack{\boldsymbol{arc} \\ \boldsymbol{without} \\ \boldsymbol{cycle\ slips}}} - \boldsymbol{c \cdot DCB_p} - \boldsymbol{c \cdot DCB^i} \right] \tag{13a}$$

In the above formula, P_1-P_2 Differential Code Biases (DCB) are assumed constant during a day, and we read them from the CODE (IGS Analysis Center) IONEX files; < > means taking the average.

Alternatively, *STEC* can be computed using P_1P_2 codes that have been smoothed with the corresponding phase,

$$\left(\boldsymbol{STEC}\right)^{\boldsymbol{i}}_{\boldsymbol{p}} = \frac{1}{\alpha 1_4} \left[\left\{ \left(\boldsymbol{P}_2\right)^{\boldsymbol{i}}_{\boldsymbol{p}} - \left(\boldsymbol{P}_1\right)^{\boldsymbol{i}}_{\boldsymbol{p}} \right\}_{\substack{\boldsymbol{smoothed} \\ \boldsymbol{with} \\ \boldsymbol{phase}}} - \boldsymbol{c \cdot DCB_p} - \boldsymbol{c \cdot DCB^i} \right] \tag{13b}$$

This leads to similar results as those obtained from Equation (13a) with respect to the same *DCB* product.

SECOND-ORDER IONOSPHERE PERTURBATIONS

Whereas the magnitude of *I1* for a given frequency depends solely on *STEC* and is always positive, the magnitude and sign of *I2* depend on the *i-p* signal direction, the actual *STEC*, and the geomagnetic field B values (Figure 3). We used the following integrated formula **[11]** in the no-bending approximation

$$\boldsymbol{I2_k = \alpha 2_k \cdot B_{IPP} \cdot \cos\theta_{B-LOS} \cdot STEC} \tag{14a}$$

with frequency factors

$$\alpha 2_3 = -\frac{7527 \cdot \boldsymbol{c}}{2 \cdot \boldsymbol{f}_1 \boldsymbol{f}_2 (\boldsymbol{f}_1 + \boldsymbol{f}_2)} \tag{14b}$$

$$\alpha 2_{1,2} = -\frac{7527 \cdot \boldsymbol{c}}{\boldsymbol{f}_{1,2}^{\ 3}} \tag{14c}$$

STEC is obtained from L_4P_4 (Equation (13a)) and B_{IPP} is computed using the accurate International Geomagnetic Reference (IGR) model **[12]**, as the latter allows us to reduce errors in *I2* up to 60% with respect to a dipolar model **[9,10]**.

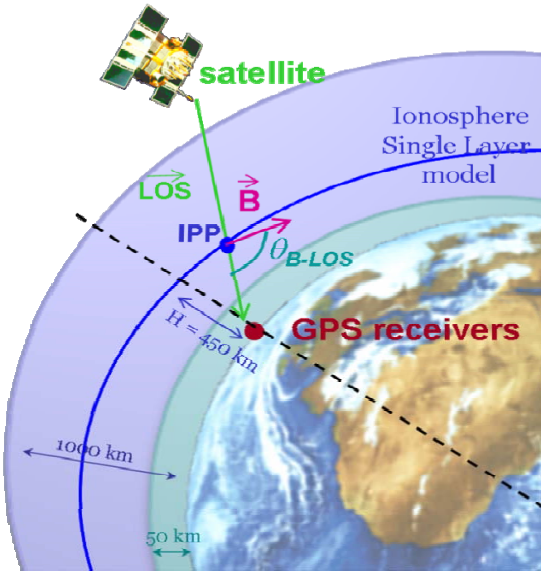

Figure 3. The third-order ionosphere effect is not only a function of STEC, but it is also function of the angle between the Line Of Sight (LOS) and the geomagnetic field B at the Ionosphere Piercing Point (IPP), and of the magnitude of B at IPP.

THIRD-ORDER IONOSPHERE PERTURBATIONS

In the ionosphere third-order contribution, the magnetic field term can be safely neglected at sub-millimeter error level, leading to the simple formula **[13]**

$$I3_k = \alpha 3_k \cdot STEC \tag{15a}$$

with frequency factors also being functions of the electronic distribution in the ionosphere:

$$\alpha 3_{1,2} = -\frac{2437 \cdot N_{\max} \cdot \eta}{f_{1,2}^{\ 4}} \tag{15b}$$

$$\alpha 3_3 = -\frac{2437 \cdot N_{\max} \cdot \eta}{3 f_1^{\ 2} \cdot f_2^{\ 2}} \tag{15c}$$

where the shape factor η is taken around 0.66 and the peak electron density along the signal propagation path, N_{max}, can determined by a linear interpolation between a typical ionosphere situation and a solar maximum one **[13,14]**:

$$N_{\max} = \frac{\left[(20-6)\cdot 10^{12}\right]}{\left[(4.55-1.38)\cdot 10^{18}\right]} \cdot \left(VTEC - 4.55 \cdot 10^{18}\right) + 20 \cdot 10^{12} \tag{16}$$

The Vertical TEC (VTEC), which is TEC along a vertical trajectory below the satellite, is taken as the projection, via the ionosphere Modified Single Layer Model mapping function, of $(STEC)^i_p$ from Equation (13a) with α_{MSLM}=0.9782, R =6371 km, H=506.7 km, as in **[15]**:

$$STEC = f_{MSLM}(z) \cdot VTEC \tag{17a}$$

$$f_{MSLM}(z) \equiv 1 \Big/ \sqrt{1 - \left(\frac{R_\oplus}{R_\oplus + H}\right)^2 \cdot \cos^2\left(\alpha_{MSLM} \cdot z\right)} \tag{17b}$$

Finally, using the above equations for the first-, second- and third-order ionosphere effects on GPS signal propagation, one finds the orders of magnitude of their impact on the code and carrier-phase measurements given in Table 1.

Table 1. Orders of magnitude of ionosphere effects I1, I2, and I3.

Orders of magnitude of ionosphere effects *I1, I2, I3* on GPS phase measurements (for codes, see converting factor in code measurement Equations (1, 3), Section 1)			
Ionosphere effect (absolute value)	**Delay in L_1L_2 per 100 TECU**	**Delay in L_3 per 100 TECU**	**Relevance [9]**

I1	*~30 ns -100 ns*	*0*	99.9% of ***I123…***
I2	*~0 – 130 ps*	*~ 0 – 45 ps*	90% of ***I23***
I3	*~0 – 3 ps*	*~ 0 – 2 ps*	

5. RESULTS

The *I2* and *I3* corrections computed according the procedure described above were applied to the ionosphere-free combinations P_3 and L_3 used in ATOMIUM. The present section shows some preliminary results: estimated second- and third-order delays on GPS signals (and on combinations of their measurements) and the impact of these on the time and frequency transfer solutions.

IONOSPHERE DELAYS

The first results concern the ionosphere perturbations in terms of delays as computed with ATOMIUM, according to the models detailed in previous section.

Firstly, recall that the Total Electron Content of the ionosphere is usually higher on average at high latitude with respect to mid-latitude stations (Figure 2). Since *I1*, *I2*, and *I3* are proportional to *Slant TEC*, the amplitude of ionosphere perturbations in GPS signal follow accordingly.

Secondly, as *TEC* reaches normally its maximal value at local noon, on a normal day, the ionosphere perturbations in GPS signal reflect this daily variation of TEC.

And finally, for any observed satellite, as the ionosphere thickness crossed by the signal is proportional to the inverse of the sine of the satellite elevation, the *STEC* during one satellite track, as well as the ionosphere delays, takes the shape of a concave curve.

Figures 4, 5, and 6 illustrate $I1_2$, $I2_3$ and $I3_3$ respectively on a quiet (left) versus an ionosphere-stormy day, the ionosphere storm of 30 November 2003 (right). The selected station in this illustration is Onsala (ONSA).

The first-order ionosphere perturbations in L_2 can reach more than 100 nanoseconds during the storm (Figures 4a and 4b), while it is less than 50 nanoseconds in normal times. *I1* in L_1 is slightly smaller according to factor f_2^2 / f_1^2. The amplitude of the *I1* effect on the codes is the same as that on the phases, but with opposite sign, as shown in Equation (1). The *I1* effect is removed from the ionosphere free combination.

The second-order ionosphere perturbation in the ionosphere-free combination (Figure 5a) is about 3 to 4 orders of magnitude smaller than the first order in L_2. $I2_3$ can reach about 20 picoseconds during the storm, about the double of its maximum value during a quiet day (Figure 5b compared to 5a).

We also recall that, in the ionosphere-free combination, the second-order ionosphere perturbation, $I2_3$, affects twice more the codes than the phases, as seen in Equation (3).

Figure 6 illustrates the third-order ionosphere perturbation, which is again an order of magnitude smaller than the second order. Here, the effect of the storm is also clear, as the third-order effect in the ionosphere-free combination can reach about 2 picoseconds during the storm (Figure 6b), while its maximum value on a non-stormy day is about 0.14 picoseconds (Figure 6a). Again, the contribution of $I3_3$ is three times more important for codes than for phases, as seen in Equation (3), but remains negligible with respect to the present precision of GPS time and frequency transfer.

IONOSPHERE IMPACT ON RECEIVER CLOCK ESTIMATES FROM A L_3P_3 ANALYSIS

Table 1 and the results presented in the above paragraph illustrate the need to take second-order ionosphere corrections into account in *P* and *L* measurements for TFT. However, to be coherent, in addition to the *I2* (and *I3*) correction(s) on GPS code and phase data, we should also use satellite orbit and clock products computed with *I2* (and *I3*) correction(s) in order to estimate the impact of the ionosphere on station clock synchronization errors via ATOMIUM. Indeed, in Reference **[11]**, it was estimated that second-order ionosphere effects in satellite clocks were the largest and could be more than 1 centimeter (i.e. ~30 picoseconds); the same authors mentioned that the second-order ionosphere effects on the satellite position are of the order of several millimeters only, and consist in a global southward shift of the constellation. Current IGS products do not take *I2* or *I3* into account. But reprocessed orbits **[16]**, taking, among others, higher-order ionosphere effects into account, are available at analysis centers **[17, 18]**. Unfortunately, they do not provide satellite clocks products. This is why we present here the impact of our ionosphere corrections on clock solutions via ATOMIUM in CV mode (Figures 7, 8, and 9), as the satellite clock is eliminated in CV. We choose the link BRUS-ONSA, i.e. Brussels-Onsala (Sweden), and the day of an ionosphere storm, 30 November 2003.

Figure 7 presents the effect of using the reprocessed orbits from **[17,18]** together with *I2* and *I3* corrections on code P_3 and phase L_3. Since satellite clocks are removed in Common-View mode, the variations are larger than what is expected (from the *I2* and *I3* delays, and from the satellite position variations due to *I2* and *I3* in reprocessed orbits). These differences could, therefore, be attributed to other differences between the IGS orbits and the processed ones.

Figure 8 shows the effect of applying the *I2* and *I3* corrections on GPS P_3L_3 analysis, without using reprocessed orbits. We see an effect up to 10 picoseconds during the ionosphere storm on the link BRUS-ONSA.

The *I3* effect shown in Figure 9 is at the present noise level of GPS observations; only a very small signal appears out of the noise during the ionosphere storm.

Consequently, in residual ionosphere perturbations in P_3L_3 (when P_3L_3 is not corrected for higher-order effects), the main contribution is $I2_3$. An *I2* delay of 20 picoseconds peak to peak during the storm (Figure 5b**)** for a given station "A" induces a variation with the corresponding differential $I2_{3A}$ - $I2_{3B}$ amplitude in CV frequency transfer with station "B", as the shape of the curve is determined by the GPS phases for which the *I2* correction is applied with a factor 1. Furthermore, *I2* induces twice as much an offset on the absolute time synchronization error (Figure 8), as the calibration of the curve is determined by the code data for which the *I2* correction is applied with a factor 2 (Equation (3)). However, this of course is still well below the present calibration capabilities of GPS equipment.

Note that the results presented here correspond to the time link BRUS-ONSA. It is, therefore, the differential ionosphere effect between those two stations (here, Brussels and Onsala) that matters for the clock solution in Common -View mode. The impact of *I2* on a clock solution in PPP could, therefore, be higher and induce larger effects on intercontinental time links. This will be investigated in further studies.

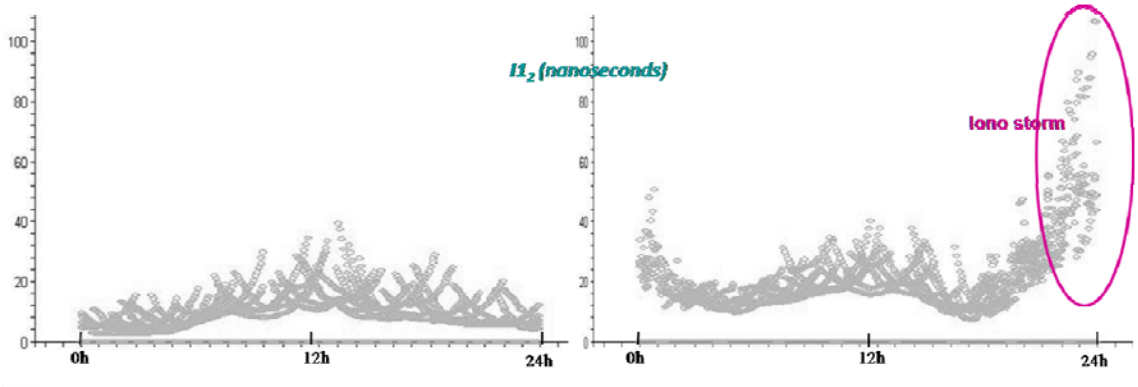

Figure 4. First-order ionosphere delay in GPS frequency 2, for station Onsala a) on an ionosphere-quiet day, 11 March 2007 (left), versus b) on an ionosphere-stormy day, 30 November 2003 (right).

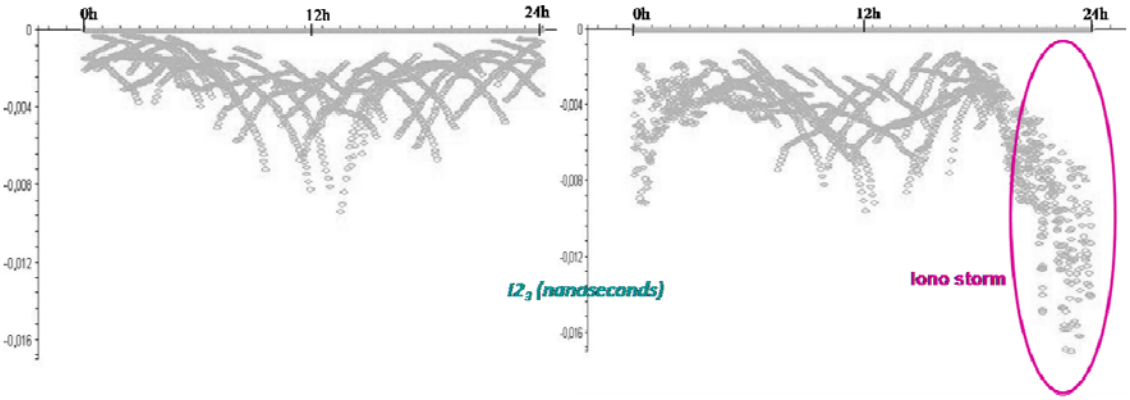

Figure 5. Second-order ionosphere delay in GPS so-called ionosphere-free combination, for station Onsala a) on an ionosphere-quiet day, 11 March 2007 (left), versus b) on a ionosphere-stormy day, 30 November 2003 (right).

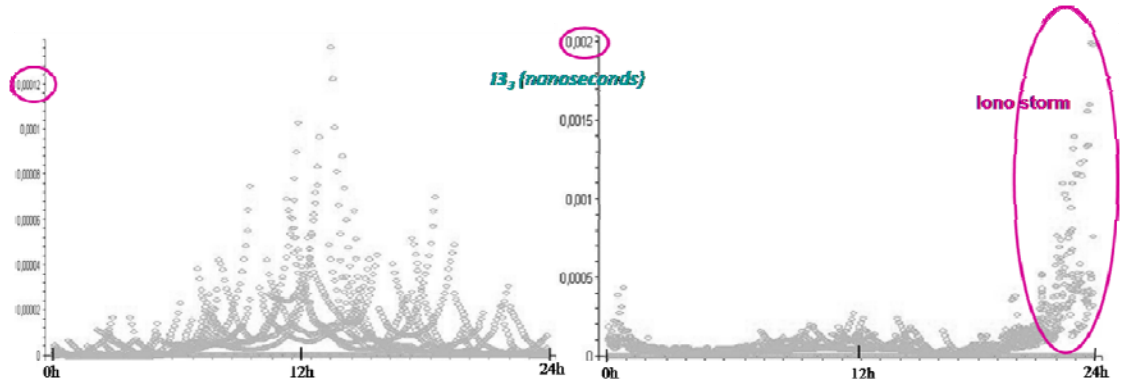

Figure 6. Third-order ionosphere delay in GPS so-called ionosphere-free combination, for station Onsala a) on an ionosphere-quiet day, 11 March 2007 (left), versus b) on an ionosphere-stormy day, 30 November 2003 (right).

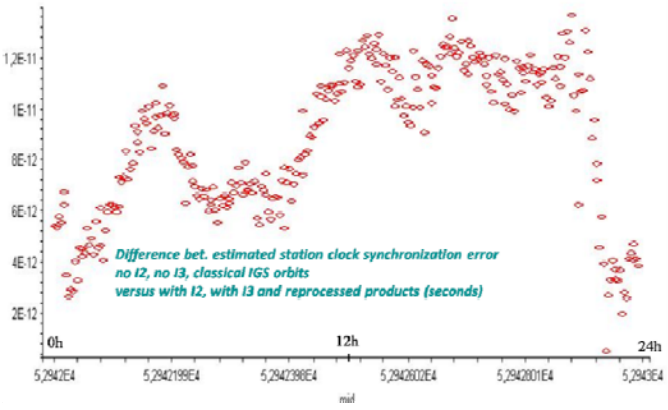

Figure 7. Effect of taking higher-order ionosphere effects into account both in the measurements and in *a-priori* products for the Brussels-Onsala link, on the ionosphere-stormy day 30 November 2007. The difference is taken between ATOMIUM-estimated station clock synchronization error when no higher-order ionosphere correction is taken into account in L_3P_3, using IGS products, versus when taking them into account together with using reprocessed products.

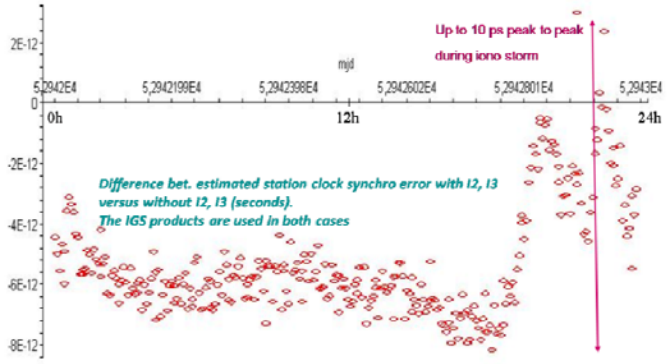

Figure 8. Effect of taking higher-order ionosphere effects, or not, into account in the L_3P_3 GPS measurements for the Brussels-Onsala link, on the ionosphere-stormy day 30 November 2007. The difference is taken between two ATOMIUM-estimated station clock solutions, both using IGS products.

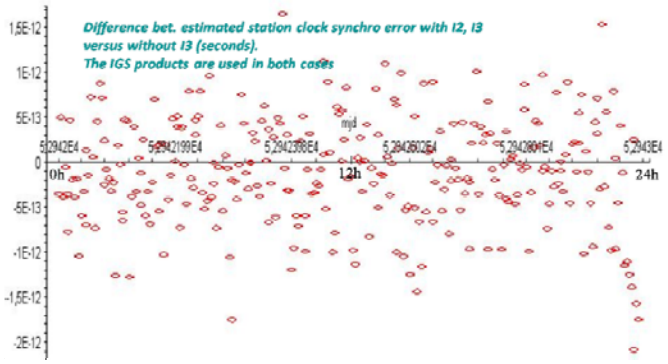

Figure 9. Effect of taking third-order ionosphere effect, or not, into account in the L_3P_3 GPS measurements for the Brussels-Onsala link, on the ionosphere-stormy day 30 November 2007. The difference is taken between two ATOMIUM-estimated station clock solutions, both using IGS products.

6. CONCLUSIONS

This study presented a least-squares analysis using the so-called ionosphere-free combination of GPS codes and phases to estimate receiver clock synchronization errors for precise frequency and time transfer. We used the ATOMIUM software, in which we implemented higher-order ionosphere contributions (second and third orders) in the ionosphere-free combination. We then compared these ionosphere residuals with the first-order ionosphere effect on the GPS dual frequency signal, which is cancelled in ionosphere-free combinations of GPS codes and phases.

It was shown that the ionosphere first-order delay of several tens of nanoseconds on an ionosphere-quiet day, is doubled in case of ionosphere storms. Though second-order delays in the ionosphere-free combination are about 3 to 4 orders of magnitude smaller than the first-order, they can reach about 20 picoseconds on a stormy day, which is relevant when performing geodetic time and frequency transfer with very stable clocks. Third-order delays in the ionosphere-free combination are yet an order of magnitude smaller, and are at the level of present noise of GPS observations.

The impact of those higher-order delays on ionosphere-free time and frequency transfer clock solutions was estimated for the time link BRUS-ONSA. It reaches more than 10 picoseconds during the ionosphere storm of 30 November 2003.

ACKNOWLEDGMENTS

This work has been supported by the Solar and Terrestrial Center of Excellence **[19]**. The authors also acknowledge the IGS for their data and products, as well as the GFZ Potsdam and TU Dresden analysis centers for their reprocessed products used in this study.

REFERENCES

[1] P. Defraigne, N. Guyennon, and C. Bruyninx, 2008, *"GPS Time and Frequency Transfer: PPP and Phase-Only Analysis,"* **International Journal of Navigation and Observation, 2008**, Article ID 175468.

[2] IGS products, *ftp://igscb.jpl.nasa.gov/*

[3] D. McCarthy and G. Petit, *"IERS Conventions 2003*, Technical Note on Displacement of Reference Points (IERS).

[4] T. Letellier, F. Lyard, and F. Lefebre, 2004, *"The new global tidal solution: FES2004,"* Jason SWT Meeting, 1-4 November 2004, St. Petersburg, Florida, USA.

[5] IGS satellite antenna phase center variations files igs01.atx and igs05.atx, *ftp://igscb.jpl.nasa.gov/pub/station/general/*

[6] J. Saastamoinen, 1972, *"Atmospheric corrections for the troposphere and stratosphere in radio ranging of satellites,"* **Geophysical Monograph 15**, Use of Artificial Satellites for Geodesy, pp. 247-251 (AGU).

[7] A. E. Niell, 1996, *"Global mapping functions for the atmospheric delay at radio wavelengths,"* **Journal of Geophysical Research, 101(B2)**, 3227-3246.

[8] J. T. Wu, S. C. WU, G.A. Hajj, W.I. Bertiger ,and S.M. Lichten, 1993, *"Effects of antenna orientation on GPS carrier phase,"* **Manuscripta Geodetica, 18**, 91-98.

[9] M. Hernandez-Pajares *et al.*, 2008, *"Methods and other considerations to correct for higher-order ionospheric delay terms in GNSS,"* presented at IGS Analysis Center Workshop, 2-6 June 2008, Miami, Florida, USA.

[10] S. Bassiri and G. A. Hajj, 1993, *"Higher-order ionospheric effects on the global positioning system observables and means of modeling them,"* **Manuscripta Geodetica. 18,** 280-289.

[11] M. Hernandez-Pajares, J. M. Juan, J. Sanz, and R. Oruz, 2007, *"Second-order ionospheric term in GPS: Implementation and impact on geodetic estimates,"* **Journal of Geophysical Research, 112, B08417**, 1-16.

[12] N. A. Tsyganenko, 2005, *"Geopack: a set of FORTRAN subroutines for computations of the geomagnetic field in the Earth's magnetosphere,"* version of 4 May 2005, available on *http://modelweb.gsfc.nasa.gov/magnetos/tsygan.html, as geopack-2005.doc* and full Fortran routines.

[13] M. Fritsche, R. Dietrich, C. Knöfel, A. Rülke, and S. Vey, 2005, *"Impact of higher-order ionospheric terms on GPS estimates,"* **Geophysical Research Letters, 32, L23311**, 1-5, Formula (14).

[14] F. K. Brunner and M. Gu, 1991, *"An improved model for the dual frequency ionospheric correction of GPS observations,"* **Manuscripta Geodetica, 16,** 205-214.

[15] R. Dach, U. Hugentobler, P. Fridez, and M. Meindl, 2007, **Bernese GPS Software**, Version 5.0, p. 259.

[16] P. Steigenberger, M. Rothacher, R. Dietrich, M. Fritsche, A. Rülke, and S. Vey, 2006, "*Reprocessing of a global GPS network,*" **Journal of Geophysical Research, 111, B05402**, 1-13.

[17] Information Systems and Data Center of GFZ Potsdam, *http://isdc.gfz-potsdam.de/gps-pdr*

[18] Technical University of Dresden, *http://www.tu-dresden.de/ipg/reprocessing.html*

[19] Solar-Terrestrial Center of Excellence (STCE), *http://www.stce.be/index.php*